

# Inhibition of NGLY1 Inactivates the Transcription Factor Nrf1 and Potentiates Proteasome Inhibitor Cytotoxicity

Frederick M. Tomlin,<sup>†,‡</sup> Ulla I. M. Gerling-Driessen,<sup>†,‡</sup> Yi-Chang Liu,<sup>†</sup> Ryan A. Flynn,<sup>†</sup> Janakiram R. Vangala,<sup>§</sup> Christian S. Lentz,<sup>||</sup> Sandra Clauder-Muenster,<sup>⊥</sup> Petra Jakob,<sup>⊥</sup> William F. Mueller,<sup>⊥</sup> Diana Ordoñez-Rueda,<sup>⊥</sup> Malte Paulsen,<sup>⊥</sup> Naoko Matsui,<sup>#</sup> Deirdre Foley,<sup>#</sup> Agnes Rafalko,<sup>#</sup> Tadashi Suzuki,<sup>¶</sup> Matthew Bogyo,<sup>||,λ</sup> Lars M. Steinmetz,<sup>⊥,§</sup> Senthil K. Radhakrishnan,<sup>§,Ⓜ</sup> and Carolyn R. Bertozzi<sup>\*,†,‡,Ⓜ</sup>

<sup>†</sup>Department of Chemistry, Stanford University, Stanford, California 94305, United States

<sup>§</sup>Department of Pathology, Virginia Commonwealth University, Richmond, Virginia 23298, United States

<sup>||</sup>Department of Pathology, Stanford University School of Medicine, 300 Pasteur Drive, Stanford, California 94305, United States

<sup>⊥</sup>Genome Biology Unit, European Molecular Biology Laboratory (EMBL), 69117 Heidelberg, Germany

<sup>#</sup>Glycomine, Inc., 953 Indiana Street, San Francisco, California 94107, United States

<sup>¶</sup>Glycometabolome Team, Systems Glycobiology Research Group, RIKEN Global Research Cluster, 2-1 Hirosawa, Wako, Saitama 351-0198, Japan

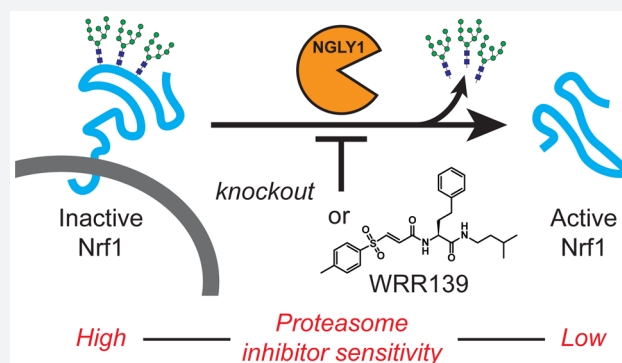
<sup>λ</sup>Department of Microbiology and Immunology, Stanford University School of Medicine, 300 Pasteur Drive, Stanford, California 94305, United States

<sup>§</sup>Department of Genetics, School of Medicine, Stanford University, Stanford, California 94305, United States

<sup>Ⓜ</sup>Howard Hughes Medical Institute, Chevy Chase, Maryland 20815, United States

## Supporting Information

**ABSTRACT:** Proteasome inhibitors are used to treat blood cancers such as multiple myeloma (MM) and mantle cell lymphoma. The efficacy of these drugs is frequently undermined by acquired resistance. One mechanism of proteasome inhibitor resistance may involve the transcription factor Nuclear Factor, Erythroid 2 Like 1 (NFE2L1, also referred to as Nrf1), which responds to proteasome insufficiency or pharmacological inhibition by upregulating proteasome subunit gene expression. This “bounce-back” response is achieved through a unique mechanism. Nrf1 is constitutively translocated into the ER lumen, N-glycosylated, and then targeted for proteasomal degradation via the ER-associated degradation (ERAD) pathway. Proteasome inhibition leads to accumulation of cytosolic Nrf1, which is then processed to form the active transcription factor. Here we show that the cytosolic enzyme N-glycanase 1 (NGLY1, the human PNGase) is essential for Nrf1 activation in response to proteasome inhibition. Chemical or genetic disruption of NGLY1 activity results in the accumulation of misprocessed Nrf1 that is largely excluded from the nucleus. Under these conditions, Nrf1 is inactive in regulating proteasome subunit gene expression in response to proteasome inhibition. Through a small molecule screen, we identified a cell-active NGLY1 inhibitor that disrupts the processing and function of Nrf1. The compound potentiates the cytotoxicity of carfilzomib, a clinically used proteasome inhibitor, against MM and T cell-derived acute lymphoblastic leukemia (T-ALL) cell lines. Thus, NGLY1 inhibition prevents Nrf1 activation and represents a new therapeutic approach for cancers that depend on proteasome homeostasis.



## INTRODUCTION

The proteasome plays an essential role in maintaining cellular homeostasis. It is responsible for the degradation of most cellular proteins in eukaryotic cells and is important for numerous processes including cell-cycle progression, apoptosis, DNA repair, and degradation of misfolded proteins derived from the

endoplasmic reticulum (ER).<sup>1–5</sup> Disrupting proteasome activity can induce an apoptotic cascade that leads to growth arrest and, subsequently, cell death.<sup>6,7</sup> Cells are particularly sensitive to

Received: May 26, 2017

Published: October 25, 2017

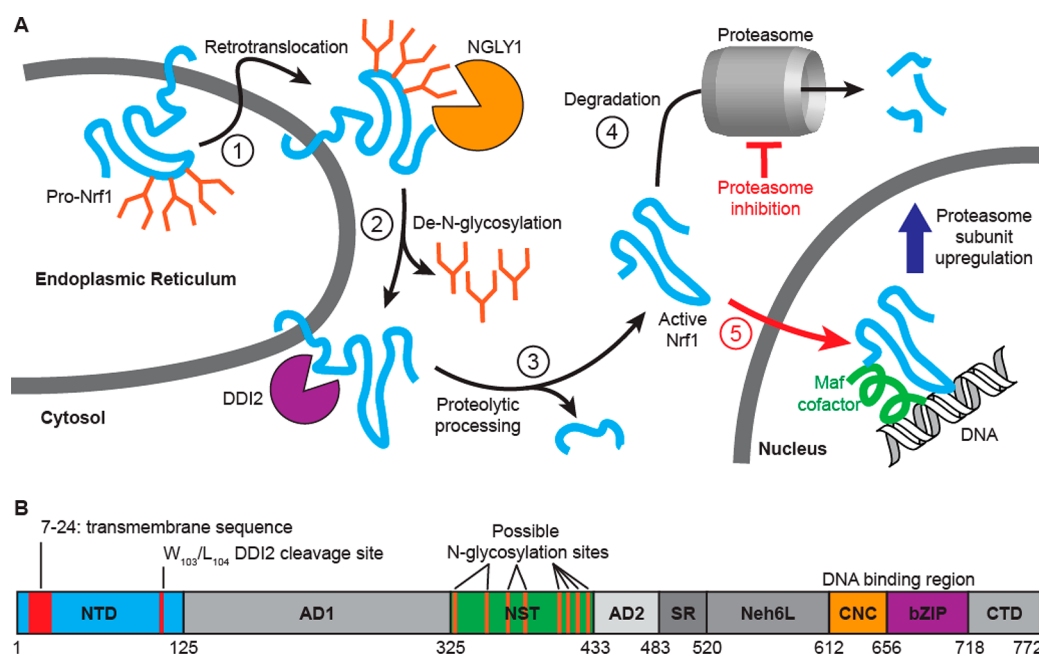


**Figure 1.** Proposed activation pathway and domain structure of Nrf1. (A) (1) Full length Nrf1 is glycosylated in the ER lumen (Pro-Nrf1) and subsequently retrotranslocated to the cytosol by VCP/p97.<sup>28</sup> (2) ER membrane-bound Pro-Nrf1 is de-N-glycosylated by NGLY1. (3) The protease DDI2 cleaves Nrf1 between W<sub>103</sub> and L<sub>104</sub> and releases the active p95 form into the cytosol. (4) Nrf1 is immediately degraded by the proteasome and thus maintained at low levels in the cell. (5) In cells with insufficient proteasome capacity due to chemical inhibition or an overload of misfolded proteins, active Nrf1 accumulates and migrates to the nucleus, where it heterodimerizes with cofactors (small Maf proteins),<sup>39</sup> binds to chromosomal targets, and activates the synthesis of PSMs. (B) Domain structure of Nrf1 with ER transmembrane domain,<sup>22</sup> site of DDI2 proteolysis, and possible N-glycosylation sites labeled in red. The N-terminal domain (NTD) contains the transmembrane sequence that anchors Nrf1 within the ER membrane and the proteolytic cleavage site for DDI2 between W<sub>103</sub> and L<sub>104</sub>. The transactivation domain (TAD) comprises the two acidic domains (AD1, AD2) and the Asn/Ser/Thr-rich region (NST) with eight predicted N-glycosylation sites (orange). The serine-rich region (SR) was found to be multiply O-GlcNAcylated, and its glycosylation status dictates the ubiquitination of the transcription factor.<sup>40</sup> The Nrf2-ECH homology 6-like domain (Neh6L) is conserved in two relatives of Nrf1, Nrf2 and Nrf3.<sup>22</sup> The DNA binding domain comprises the cap 'n' collar (CNC) and the basic leucine zipper domain (bZIP), which enable heterodimerization with Maf proteins before binding to the DNA. The C-terminal domain (CTD) also contributes to transcription factor activity.<sup>34</sup>

proteasome inhibition if their proteasome capacity is near saturation due to a heavy protein degradation load,<sup>8,9</sup> or if their survival hinges on rapid turnover of key protein factors.<sup>6,10–12</sup> These situations arise in various cancers, and thus the proteasome has become an important drug target in oncology.<sup>13–15</sup>

Bortezomib, a dipeptidyl boronic acid derivative that reversibly targets the active site of the  $\beta 5$ -subunit of the 20S proteasome, was the first FDA approved proteasome inhibitor for oncology.<sup>16</sup> This drug has been particularly effective in treatment of multiple myeloma (MM) and mantle cell lymphoma (MCL), albeit with side effects such as peripheral neuropathy and gastrointestinal distress that have been attributed, in part, to off-target effects.<sup>15,16</sup> The search for more potent and selective drugs led to second-generation proteasome inhibitors such as the epoxyketone carfilzomib,<sup>17</sup> which has also been approved for use in treating MM.<sup>18</sup> Although these medicines have improved the outcomes of patients with MM and MCL, a high frequency of both inherent and acquired resistance has limited their impact.<sup>15,19</sup> In addition, to date, proteasome inhibitors have met with little success in the treatment of solid tumors.<sup>20</sup>

Resistance to proteasome inhibition is thought to arise from upregulation of proteasome subunit (PSM) levels, from enhanced proteasome assembly efficiency, or through other mechanisms that enhance proteasome activity.<sup>15</sup> A potential contributor to proteasome inhibitor drug resistance is the transcription factor Nuclear Factor, Erythroid 2 Like 1

(NFE2L1), which is also referred to as NF-E2-related factor 1 (Nrf1).<sup>21</sup> (There is an unrelated transcription factor, nuclear respiratory factor 1, which also bears the abbreviation Nrf1 but should not be confused with the Nrf1 described here.) Nrf1 is a member of the “cap 'n' collar” bZIP transcription factor family and is a regulator of various metabolic pathways, such as lipid and amino acid metabolism, the transactivation of antioxidant enzymes, bone formation, and the maintenance of proteostasis.<sup>22</sup> Importantly, Nrf1 is capable of upregulating PSM gene expression.<sup>23</sup> The DNA sequence targeted by Nrf1 is called the antioxidant response element (ARE), which is also recognized by the other Nrf family members Nrf2 and Nrf3.<sup>24–27</sup>

A unique feature of Nrf1 is its complex posttranslational regulation (shown schematically in Figure 1A).<sup>28</sup> Nrf1 is cotranslationally targeted to the ER and is inserted into the ER membrane as an N-glycosylated transmembrane protein. Perhaps unique among transcription factors, the major portion of Nrf1, including its C-terminal DNA-binding domain, initially resides within the ER lumen. Nrf1 is constitutively targeted for retrotranslocation to the cytosol and proteasomal degradation via the ER-associated degradation (ERAD) pathway.<sup>28</sup> The protein is thereby maintained at low basal levels.<sup>29</sup> However, when proteasome capacity is saturated, such as by an overload of misfolded proteins or by treatment with proteasome inhibitors, retrotranslocated Nrf1 accumulates in the cytosol, where it is activated by posttranslational processing, traffics to the nucleus, and activates its target genes in partnership with small Maf

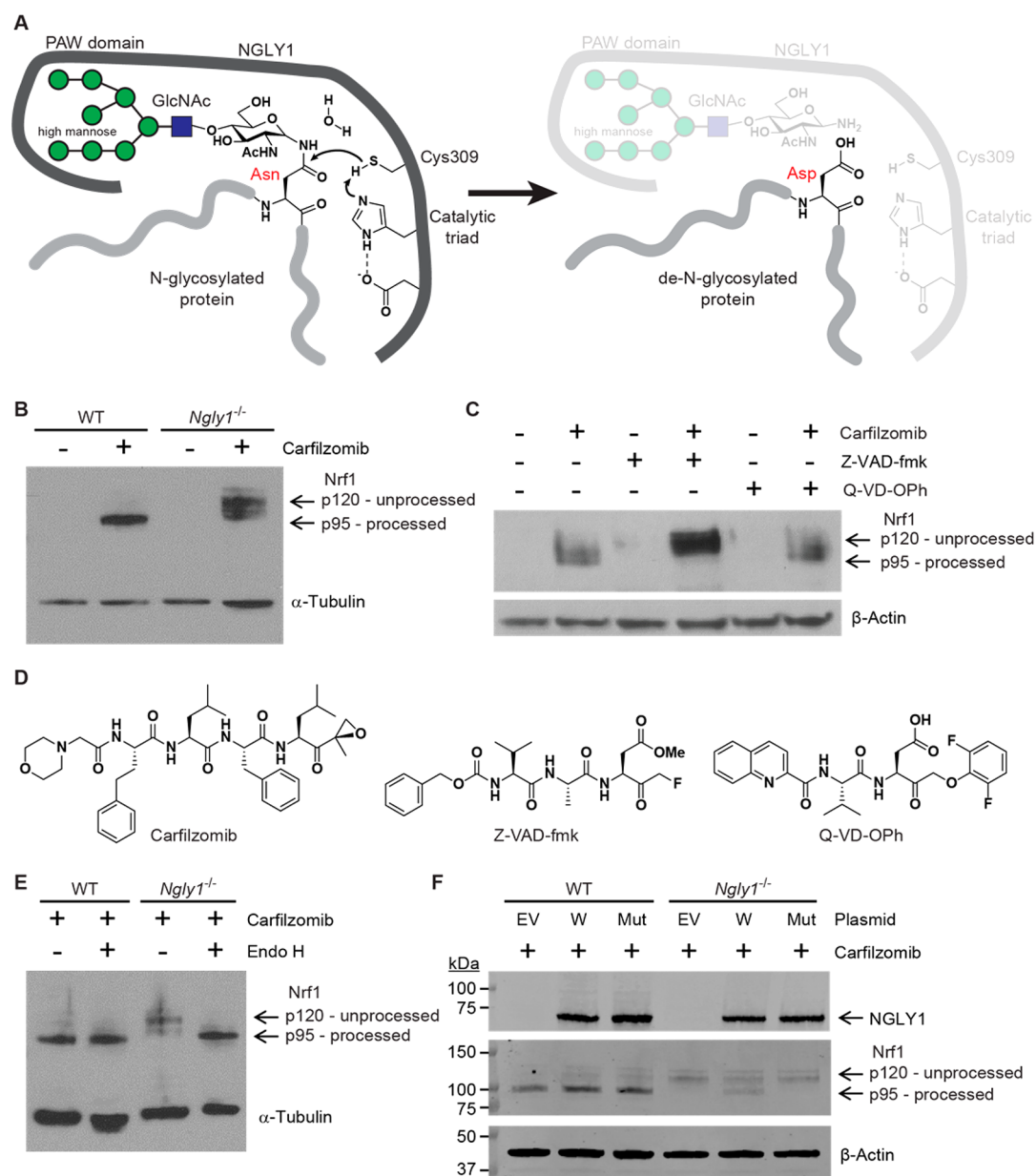


**Figure 2.** Nrf1 processing is altered by genetic or chemical disruption of NGLY1 activity. (A) Schematic of the mechanism of N-glycan cleavage by NGLY1 (dark gray). (B) WT and *Ngly1*<sup>-/-</sup> MEFs were treated with the proteasome inhibitor carfilzomib (100 nM) for 2 h prior to harvest, cell lysis, and subsequent immunoblotting. Nrf1 was visualized by incubating the blot with a monoclonal antibody raised against the region surrounding aa129, followed by a HRP-conjugated secondary antibody. The unprocessed and glycosylated form of Nrf1 is seen as multiple bands between 100 and 120 kDa (p120) whereas de-N-glycosylated processed Nrf1 appears at approximately 95 kDa (p95). (C) HEK293 cells overexpressing human Nrf1 engineered with a C-terminal 3xFLAG-tag were treated with the NGLY1 inhibitor Z-VAD-fmk (20 μM) or the pan-caspase inhibitor Q-VD-OPh (50 nM) for 5 h prior to treatment with carfilzomib (100 nM) for another 2 h. The cells were allowed to recover in fresh medium for 2 h and then lysed and analyzed by immunoblotting as above. (D) Chemical structures of carfilzomib, a proteasome inhibitor; Z-VAD-fmk, an NGLY1 inhibitor with pan-caspase inhibitor activity; Q-VD-OPh, a pan-caspase inhibitor that does not inhibit NGLY1. (E) WT and *Ngly1*<sup>-/-</sup> MEFs were treated with the proteasome inhibitor carfilzomib (200 nM) for 12 h prior to harvest, cell lysis, denaturation, and treatment with Endo H (15000 U) for 16 h before immunoblotting as in 2B. (F) WT and *Ngly1*<sup>-/-</sup> MEFs were treated with a premixed solution of plasmid DNA and Lipofectamine 2000 for 44 h. The medium was replaced with fresh medium containing carfilzomib (50 nM) for an additional 4 h. The cells were washed, harvested, and lysed before analysis by immunoblotting with anti-NGLY1 and anti-Nrf1 primary antibodies. EV: empty vector. W: wild-type NGLY1. Mut: NGLY1 C309S.

proteins. Thus, Nrf1 is thought to mediate a “bounce-back” response that balances proteasome load and capacity, thereby maintaining proteostasis.<sup>23</sup> Accordingly, Nrf1 could undermine the efficacy of proteasome inhibitors and may influence their performance as cancer therapies.

Disrupting the action of Nrf1 could, in principle, potentiate proteasome inhibitor activity. But as a transcription factor, Nrf1

is not an attractive drug target.<sup>30</sup> However, its activity is dependent on discrete processing events that include de-N-glycosylation and partial proteolytic cleavage of an approximately 120 kDa (p120) precursor to give rise to the active form of approximately 95 kDa (p95).<sup>23,31</sup> (The active form of Nrf1 has also been annotated at p110 in previous reports.<sup>23</sup> Here it was observed at p95, and thus this naming convention was used. In all



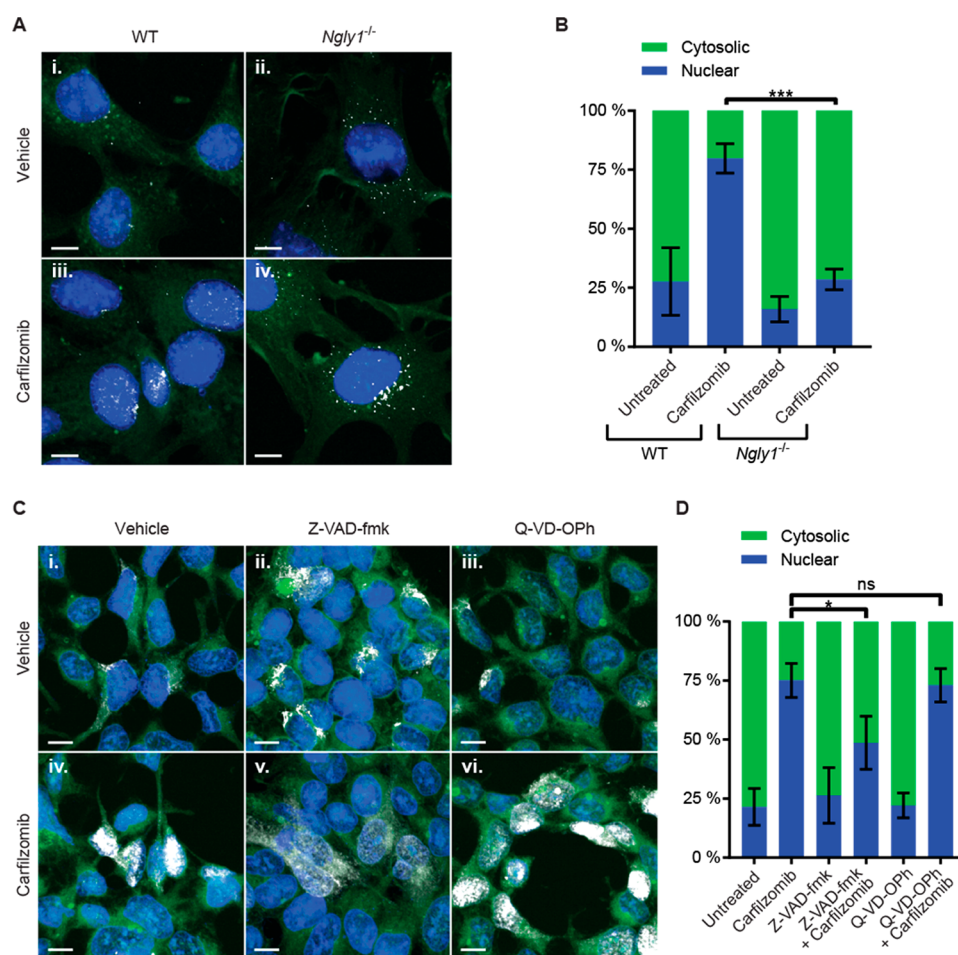


**Figure 3.** Loss of NGLY1 activity reduces nuclear localization of Nrf1 in response to carfilzomib treatment. (A) Immunofluorescence microscopy of WT and *Ngly1*<sup>-/-</sup> MEFs grown on coverslips and treated with carfilzomib or vehicle for 2 h. The cells were recovered in fresh medium for 1 h prior to fixation and imaging. Cells were incubated with a polyclonal antibody recognizing the middle region of Nrf1 (aa 191–475) followed by an Alexa Fluor 647 conjugated secondary antibody. Nrf1 immunoreactivity is indicated in white, autofluorescence is shown in green, and DAPI stained nuclei are in blue. (i, ii) Vehicle-treated WT and *Ngly1*<sup>-/-</sup> MEFs, respectively. (iii, iv) Carfilzomib (100 nM)-treated WT and *Ngly1*<sup>-/-</sup> MEFs, respectively. (B) Quantitation of Nrf1 staining was accomplished by calculating the overlap of the white channel (Nrf1) with the blue channel (nucleus) and comparing it to the overall Alexa Fluor 647 signal, which was set to 100%. The difference gave the amount of Nrf1 staining outside the nucleus (green bar) and inside the nucleus (blue bar). Quantitation was performed using 4 images (125 × 75 μm) per condition and averaged. (C) Immunofluorescence microscopy images of HEK293 cells overexpressing human C-terminal 3xFLAG-tagged Nrf1 that were treated with NGLY1 inhibitor Z-VAD-fmk or the caspase inhibitor Q-VD-OPh for 5 h prior to treatment with carfilzomib. (i, ii, iii) Cells with no treatment, Z-VAD-fmk (100 μM), or Q-VD-OPh (50 nM). (iv, v, vi) Cells treated as panels i, ii, and iii with carfilzomib (20 nM, 2 h). The cells were recovered in fresh medium for 1 h prior to fixation and imaging. (D) Quantitation of Nrf1 staining was performed using 4 images (125 × 75 μm) per condition and averaged, as described in panel B. Scale bars = 10 μm. Error bars represent one standard deviation from the mean. \**p* < 0.05, \*\*\**p* < 0.0005, ns = not significant.

cases, the active form of Nrf1 has been observed to have a lower molecular weight compared to the ER-resident immature form.) The enzymes that mediate these processing events are emerging as possible alternative targets for disruption of Nrf1 activity. Ruvkun<sup>32</sup> and Murata<sup>33</sup> and their respective co-workers recently discovered that aspartyl protease DNA-damage inducible 1 homologue 2 (DDI2) is responsible for cleaving the N-terminal transmembrane sequence and releasing Nrf1 from the ER membrane. Here, we focus on defining the significance of de-N-glycosylation with regard to Nrf1 activation.

N-glycosylation of Nrf1 is thought to occur within an “NST” domain that includes eight potential N-glycosites (see Figure 1B for a detailed description of Nrf1’s domain architecture). Hayes and co-workers speculated that deglycosylation of the NST domain, with concomitant conversion of Asn to acidic Asp residues, would create a functional transactivating domain (TAD) required for transcriptional activation.<sup>34</sup> Indeed, they

found that mutation of the potential N-glycosites from Asn to Asp enhanced the ability of Nrf1 to activate transcription in a reporter gene assay. This observation, combined with the finding that Nrf1 activation involves its processing from the p120 to the deglycosylated p95 form upon proteasome inhibition,<sup>23,28</sup> suggests that de-N-glycosylation activity is required for Nrf1 function.

The mammalian enzyme responsible for removing N-glycans from proteins in the cytosol is N-glycanase 1 (PNGase, NGLY1 in humans, *Ngly1* in mice).<sup>35–37</sup> Although a role for this enzyme in Nrf1 activation has not been directly demonstrated, a recent gene essentiality profile in 14 human leukemia cell lines uncovered a correlated essentiality of Nrf1, NGLY1, and DDI2, suggesting that they function in a common pathway.<sup>38</sup> Compellingly, in a forward genetic screen, Ruvkun and co-workers identified the *Caenorhabditis elegans* NGLY1 orthologue PNG1 as essential for activity of its Nrf1 orthologue SKN1.<sup>32</sup>



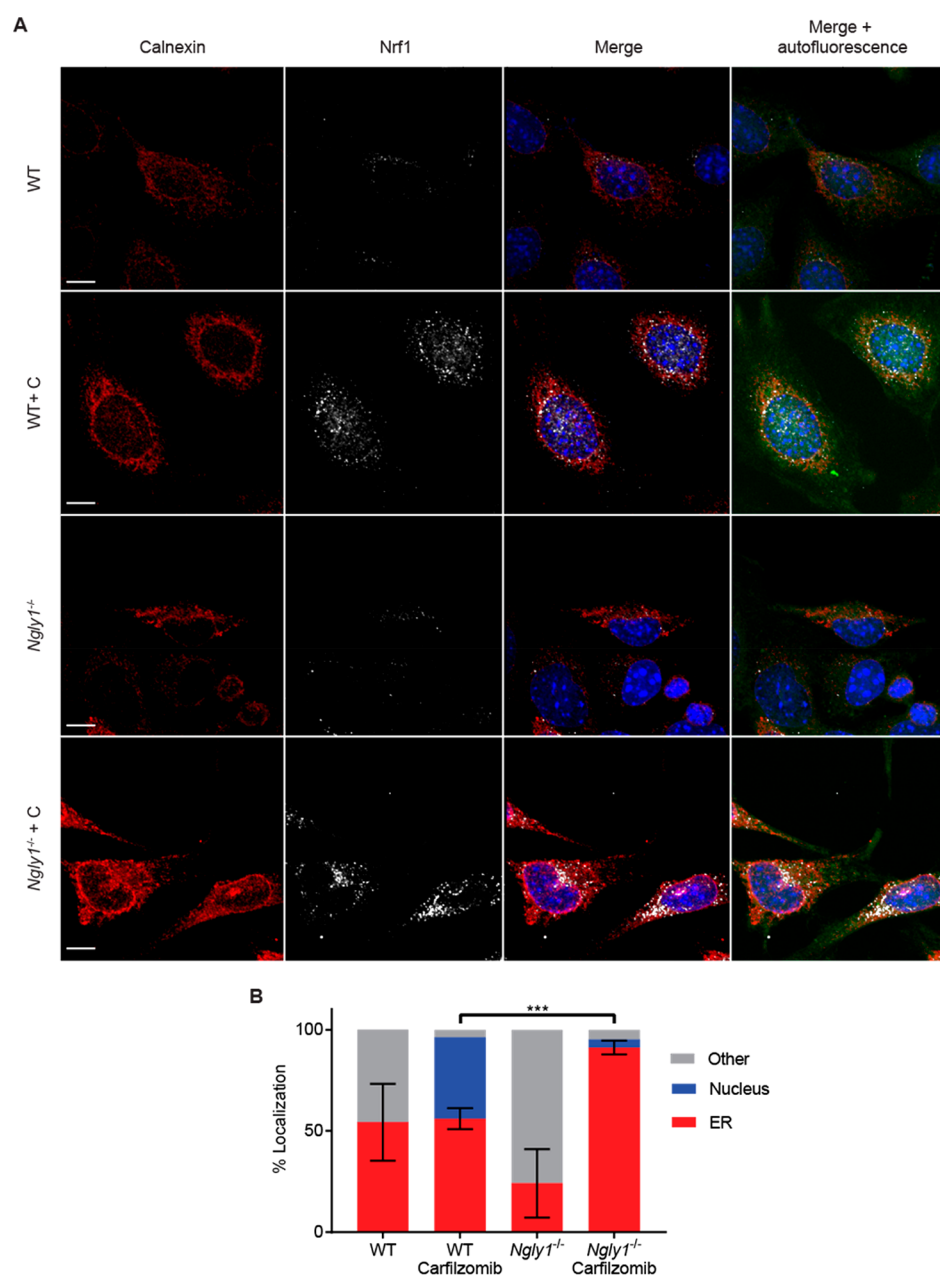


**Figure 4.** Immunofluorescence staining of Nrf1 in WT or *Ngly1*<sup>-/-</sup> MEFs with or without treatment with carfilzomib. (A) MEFs (WT or *Ngly1*<sup>-/-</sup>) were treated with vehicle or carfilzomib (100 nM) and stained for calnexin (red, ER localized), Nrf1 (white), and DAPI (blue), as described in Figure 3. Autofluorescence (green) is shown for full cell visualization. (B) Quantitation of Nrf1 localization was done by calculating the overlap of the white channel (Nrf1) with the blue (nucleus) or red (calnexin/ER) channels and comparing it to the overall Nrf1 signal, which was set to 100%. Quantitation was performed in 4 images (125 × 75 μm) per condition and averaged. Scale bars = 10 μm. Error bars represent one standard deviation from the mean with regard to ER overlap. \*\*\**p* < 0.0005.

Furthermore, the PNG1 mutant worm was sensitized to proteasome inhibitor toxicity. These results support the notion that interfering with Nrf1 processing enzymes may potentiate proteasome inhibitor activity.

Here, we demonstrate that functional NGLY1 is essential for Nrf1 processing, nuclear translocation, and transcription factor activity. Furthermore, through a targeted library screening approach, we discovered a small molecule inhibitor of NGLY1 that enhances the cytotoxicity of proteasome inhibition in cancer cell lines. These findings implicate NGLY1 as a possible target for cancer therapy in conjunction with proteasome inhibition.

## RESULTS

**NGLY1 Is Critical for the Processing, Subcellular Localization, and Transcriptional Activity of Nrf1.** First discovered by Suzuki and co-workers, human NGLY1 is thought to be responsible for removing N-glycans from misfolded ERAD substrates.<sup>41</sup> The enzyme catalyzes hydrolysis of the amide bond between the proximal *N*-acetylglucosamine (GlcNAc) residue and the Asn side chain to which it is attached (Figure 2A). NGLY1's catalytic mechanism is likely similar to that of a cysteine protease.<sup>42,43</sup> It possesses a canonical Cys-His-Asp catalytic triad where Cys<sub>309</sub> serves as the reactive nucleophile.<sup>43</sup> Upon de-N-glycosylation of the protein, the Asn residue is converted to Asp

and a 1-amino-GlcNAc-containing free oligosaccharide is released. In addition to its catalytic domain, NGLY1 has a C-terminal carbohydrate-binding “PAW domain” that recognizes high mannose-type glycans typically present on proteins selected for ERAD.<sup>43,44</sup> NGLY1 also possesses an N-terminal “PUB domain” that interacts with p97, a component of the retrotranslocation machinery.<sup>45,46</sup>

In order to test the hypothesis that NGLY1 is required for the correct processing of Nrf1, we evaluated conversion of the p120 to p95 forms in wild type (WT) mouse embryonic fibroblasts (MEFs) and those derived from *Ngly1*<sup>-/-</sup> mice.<sup>47</sup> As shown by the immunoblot in Figure 2B, treatment of WT MEFs with carfilzomib (Figure 2D) led to an accumulation of Nrf1 in the p95 form. By contrast, in the *Ngly1*-null background, carfilzomib induced Nrf1 accumulation but in abnormally processed forms (multiple bands from 100 to 120 kDa, hereafter referred to collectively as p120). Similar observations were made using Nrf1-overexpressing HEK293 cells in which NGLY1 was chemically inhibited. We used the thiol-reactive compound Z-VAD-fluoromethylketone (fmk) (Figure 2D) which is best known as a potent pan-caspase inhibitor but was discovered by Korbel et al. to block NGLY1 as well.<sup>48</sup> Incubation of the HEK293 cells with Z-VAD-fmk prior to treatment with carfilzomib led to misprocessing of Nrf1 similar to that observed in *Ngly1*<sup>-/-</sup> MEFs (Figure 2C). The high abundance of the p120 bands in cells treated with Z-VAD-fmk indicates that the N-glycosylated form of Nrf1 is the dominant species. By contrast, another pan-caspase inhibitor Q-VD-OPh (Figure 2D), which does not act on NGLY1,<sup>48</sup> did not impair processing of Nrf1 compared to untreated cells (Figure 2C). To confirm that the change from p120 to p95 is the result of the removal of N-glycans, WT and *Ngly1*<sup>-/-</sup> MEFs were treated with carfilzomib, harvested, and lysed. These lysates were then treated with Endo H to remove any remaining high-mannose glycans (Figure 2E, full Western blot shown in Figure S1). While Nrf1 in WT cells remained at p95, the p120 bands in *Ngly1*<sup>-/-</sup> lysates were reduced to a single band at p95 after treatment with Endo H, indicating that these bands are made up of Nrf1 with varying amounts of N-glycosylation. To demonstrate that catalytically active NGLY1 is required for the removal of these N-glycans from Nrf1, WT and *Ngly1*<sup>-/-</sup> MEFs were transfected with native and catalytically dead point mutant human NGLY1 (Figure 2F). Only catalytically active NGLY1 was able to partially restore Nrf1 processing after carfilzomib treatment, while catalytically dead NGLY1 C309S did not restore processing of Nrf1. Thus, removal of N-glycans from Nrf1 appears to be dependent on the catalytic activity of NGLY1. These data show that genetic or chemical disruption of NGLY1 activity leads to aberrant processing of Nrf1.

In order for Nrf1 to initiate gene expression it must translocate to the nucleus. Thus, we investigated whether Nrf1's subcellular distribution was perturbed in the absence of NGLY1 activity. Using immunofluorescence microscopy, we analyzed the localization of Nrf1 in WT and *Ngly1*<sup>-/-</sup> MEFs as well as Nrf1-overexpressing HEK293 cells, both before and after carfilzomib treatment (Figure 3). In the absence of carfilzomib, WT and *Ngly1*<sup>-/-</sup> MEFs show Nrf1 immunoreactivity (white) in low abundance and mainly outside of the nucleus (Figure 3A,B). This non-nuclear staining could be cytosolic and/or associated with the ER membrane (*vide infra*). After treating the cells with carfilzomib, Nrf1 staining in WT MEFs was redistributed predominantly to the nucleus. By contrast, carfilzomib-treated *Ngly1*<sup>-/-</sup> MEFs retained the majority of Nrf1 immunoreactivity

outside the nucleus. The same effect was observed in the Nrf1-overexpressing HEK293 cells (Figure 3C,D). Untreated HEK293 cells showed the majority of Nrf1 staining outside the nucleus. After incubation with carfilzomib, Nrf1 staining shifted to a largely nuclear localization. However, inhibition of NGLY1 with Z-VAD-fmk prior to incubation with carfilzomib reduced the proportion of nuclear Nrf1 staining compared to cells without NGLY1 inhibitor (Figure 3C,D). By contrast, Q-VD-OPh treatment had no effect on Nrf1's subcellular distribution.

We noticed that extranuclear Nrf1 staining in *Ngly1*<sup>-/-</sup> MEFs was not uniformly distributed. Rather, the staining appeared as puncta situated proximal to the nucleus. This observation led us to perform colocalization studies with the ER marker calnexin in WT and *Ngly1*<sup>-/-</sup> MEFs treated with carfilzomib (Figure 4). In proteasome-inhibited WT MEFs, Nrf1 staining was evenly distributed between the ER and nucleus. This contrasted with proteasome-inhibited *Ngly1*<sup>-/-</sup> MEFs, in which >90% of Nrf1 staining colocalized with the ER marker. The apparent discrepancy in quantity of nuclear localization between WT MEFs treated with carfilzomib in Figure 3B (75%) and Figure 4B (45%) may be due to increased precision of quantitation afforded by an ER marker. These microscopy data indicate that, in the absence of *Ngly1* activity, Nrf1 accumulates outside the nucleus and is likely associated with the ER membrane. This observation is consistent with the proposed processing pathway shown in Figure 1A.

In light of the observations that Nrf1 is misprocessed and mislocated without de-N-glycosylation by NGLY1, we suspected that its transcriptional activity would also be impaired. To test this, we used two functional assays previously used to probe Nrf1 activation in response to proteasome inhibition.<sup>23</sup> The first was a luciferase reporter assay that measures transcription of genes under control of the antioxidant response element (ARE) derived from the gene encoding the human proteasome subunit PSMA4. WT and *Ngly1*<sup>-/-</sup> MEFs transiently transfected with ARE luciferase reporter plasmid were treated with carfilzomib or vehicle for 12 h. Subsequently, the cells were treated with luciferin and bioluminescence was measured and normalized to the expression of renilla luciferase that served as an internal control (Figure 5A). Only WT cells showed an increase in bioluminescence after carfilzomib treatment, while the *Ngly1*<sup>-/-</sup> cells showed no response to proteasome inhibition. The same experiment was performed in Nrf1-overexpressing HEK293 cells using Z-VAD-fmk to chemically inhibit NGLY1 prior to incubation with carfilzomib (Figure 5B). Q-VD-OPh served as a caspase inhibition control. Cells incubated with Z-VAD-fmk showed no enhancement of luciferase activity in response to proteasome inhibition, whereas vehicle- and Q-VD-OPh-treated cells showed enhanced bioluminescence.

The second test of Nrf1 function was a qPCR assay measuring the relative levels of PSM mRNAs after treatment of cells with proteasome inhibitors.<sup>23</sup> WT and *Ngly1*<sup>-/-</sup> MEFs were treated with carfilzomib for 12 h and lysed, and relative levels of mRNAs corresponding to PSMA7, PSMB7, and PSMC4 were determined by qPCR (Figure 5C). All three mRNAs were elevated by carfilzomib treatment in WT MEFs, but remained unchanged in *Ngly1*<sup>-/-</sup> MEFs. Collectively, the data shown thus far indicate that the processing, subcellular localization, and activity of Nrf1 are all impaired in cells lacking functional NGLY1. Thus, genetic or chemical inhibition of NGLY1 undermines the proteasome bounce-back response mediated by Nrf1.

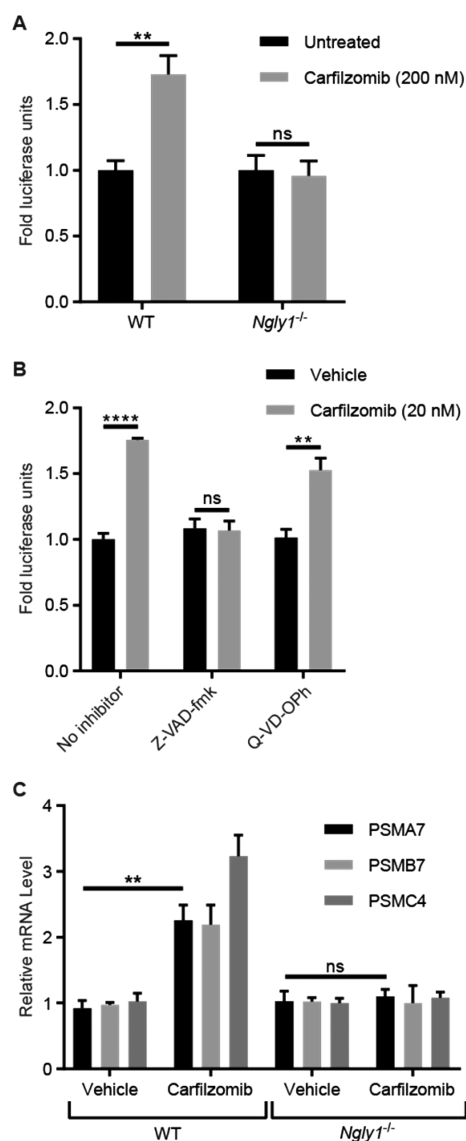


**Figure 5.** NGLY1 activity is required for Nrf1 to initiate the proteasome bounce-back response. (A) WT and *Ngly1*<sup>-/-</sup> MEFs were transiently transfected overnight with a plasmid expressing firefly luciferase under the control of three copies of the human antioxidant response element (ARE). The next day, the cells were treated with carfilzomib (200 nM) for 12 h and bioluminescence was measured. (B) HEK293 cells overexpressing human C-terminal 3xFLAG-tagged Nrf1 were transfected with the same reporter plasmid overnight and then treated with Z-VAD-fmk (20  $\mu$ M) or Q-VD-OPh (50 nM) for 5 h prior to treatment with carfilzomib (20 nM) for 12 h. Bioluminescence was then measured. (C) WT and *Ngly1*<sup>-/-</sup> MEFs were treated with carfilzomib (200 nM) for 12 h. mRNAs corresponding to proteasome subunits PSMA7, PSMB7, and PSMC4 were quantitated by qPCR. Statistical significance is similar for each qPCR measurement between WT and *Ngly1*<sup>-/-</sup> MEFs. Error bars represent one standard deviation. \*\* $p < 0.005$ , \*\*\*\* $p < 0.00005$ , ns = not significant.

### Genetic Inactivation of NGLY1 Increases Sensitivity of Cells to Proteasome Inhibitor Cytotoxicity.

The Nrf1-mediated proteasome bounce-back response is known to undermine proteasome inhibitor cytotoxicity in cancer cell lines.<sup>23</sup> Therefore, we sought to test the effects of NGLY1 disruption on proteasome inhibitor sensitivity. We treated *Ngly1*<sup>-/-</sup> and WT MEFs with increasing amounts of carfilzomib for 24 h and measured their viability using the commercial

CellTiter-Glo 2.0 Assay (Figure S2). *Ngly1*<sup>-/-</sup> cells were significantly more sensitive to treatment with carfilzomib than their WT counterparts. The reduction in survival corresponded to a 3-fold decrease in the LD<sub>50</sub> of carfilzomib in *Ngly1*<sup>-/-</sup> compared to WT MEFs.

To test whether loss of NGLY1 activity in human cells enhances carfilzomib's potency, we applied CRISPRi to knockdown Nrf1 or NGLY1 in two model cell lines. K562 and HeLa cells expressing a dCas9-KRAB construct were stably transduced with single-guide RNAs (sgRNAs) targeting the transcription start sites of *Nrf1* or *NGLY1*. The sgRNA allows the dCas9-KRAB construct to bind to and suppress transcription of the target gene. A nontargeting sgGAL4-4 was used as the negative control.<sup>49</sup> The extent of the knockdowns was determined by qPCR analysis of the transcripts (Figure S3A,B) as well as western blot to confirm lowered protein levels (Figure S3C,D). The knockdown cells were then assayed for survival in the presence of carfilzomib (Figure 6A,B). With control sgRNA,

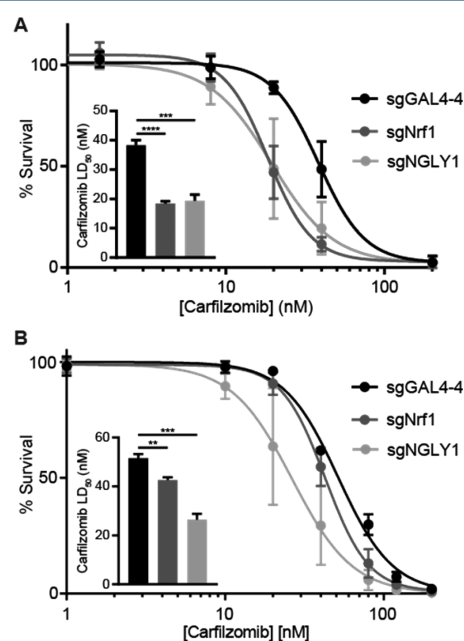


**Figure 6.** NGLY1 knockdown increases sensitivity of cells to carfilzomib. K562 (A) and HeLa (B) cells transduced with sgGAL4-4, sgNrf1, or sgNGLY1 were treated with carfilzomib for 48 h, and their viability was compared to vehicle-treated cells using the CellTiter-Glo assay. Cell survival assays were performed with 3 and 4 replicates for K562 and HeLa cells, respectively. Error bars represent one standard deviation from the mean. Inset: The LD<sub>50</sub>s of carfilzomib for K562 and HeLa cells were calculated by 4-variable nonlinear regression. Error bars represent standard error. \*\* $p < 0.005$ , \*\*\* $p < 0.0005$ , \*\*\*\* $p < 0.00005$ .

the LD<sub>50</sub>s of carfilzomib for K562 and HeLa cells were 40 and 50 nM, respectively. In the Nrf1- or NGLY1-knockdown cells (sgNrf1 or sgNGLY1), carfilzomib's LD<sub>50</sub>s were up to 2-fold lower for both cell lines. The magnitude of this effect is consistent with previous observations using proteasome inhibitors in the presence of Nrf1 shRNA knockdown.<sup>23</sup> Our data show that knockdown of NGLY1 has a similar or greater effect on carfilzomib potency compared to knockdown of Nrf1.

### Discovery of a New Small Molecule Inhibitor of NGLY1.

Since NGLY1 knockdown potentiates proteasome inhibitor toxicity, a small molecule NGLY1 inhibitor may have therapeutic value in combination with drugs like carfilzomib. Although Z-



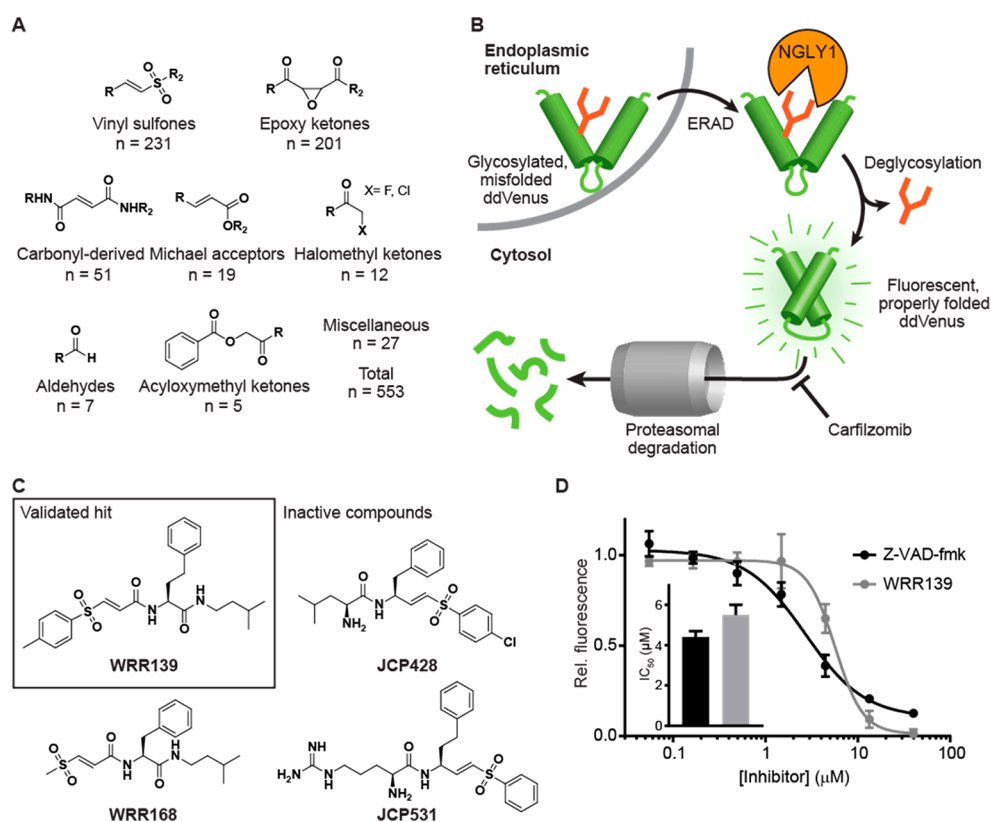


**Figure 7.** A targeted screen of thiol-reactive compounds led to the discovery of novel NGLY1 inhibitor WRR139. (A) Warhead variety represented in the 553-compound library. (B) Schematic of the modified Cresswell assay. K562 cells stably express a fluorescent Venus protein with a mutated asparagine N-glycosylation site (ddVenus). Upon translation, the protein is N-glycosylated, preventing proper folding and thus fluorescence. The glycosylated ddVenus is shuttled through the ERAD pathway, and upon de-N-glycosylation the mutated Asn is converted to Asp, allowing proper folding and thus fluorescence. A proteasome inhibitor is needed to prevent immediate degradation of the fluorescent ddVenus. Inhibition of NGLY1 in this cellular assay decreases fluorescence by preventing proper folding of ddVenus. (C) Structure of the hit WRR139 as well as related compounds that did not show activity in the assay. (D) K562 cells expressing ddVenus were incubated with carfilzomib (1  $\mu\text{M}$ ) and either WRR139 or Z-VAD-fmk for 6 h. Fluorescence was measured by flow cytometry and compared to cells treated with only carfilzomib. Error bars represent one standard deviation from the mean.

VAD-fmk inhibits NGLY1 in cultured cells, it is not a good tool compound for studies of this kind due to its off-target pan-caspase inhibitor activity. Based on a prior report, Z-VAD-fmk should irreversibly inhibit all caspases in less than an hour at concentrations under 1  $\mu\text{M}$ .<sup>50</sup> Indeed, cotreatment of U266 multiple myeloma cells with Z-VAD-fmk and carfilzomib was less toxic than treatment with carfilzomib alone (Figure S4). We anticipated this result as the main mechanism of cell death from proteasome inhibition is apoptosis and caspases are essential for that process.<sup>51</sup> Thus, we sought to develop a new NGLY1 inhibitor lacking such off-target activity.

The mechanism of NGLY1 is like that of a cysteine protease, wherein a nucleophilic cysteine residue within a catalytic triad attacks the amide carbonyl of the glycosylated asparagine side chain (Figure 2A).<sup>41</sup> This mechanism underlies the cross-inhibitory activity of Z-VAD-fmk with the caspases and NGLY1. Previous work identified specific inhibitors of NGLY1 based on a chitobiose core armed with an electrophilic warhead, but these are either not cell permeable or synthetically complicated.<sup>42,52,53</sup> We hypothesized that alternative drug-like NGLY1 inhibitors might be discovered by screening a library of peptide-based thiol-reactive electrophiles.<sup>54–60</sup> Accordingly, we focused on a collection of  $\sim 600$  compounds bearing vinyl sulfones, epoxy ketones, various Michael acceptors, halomethyl ketones, aldehydes, and acyloxymethyl ketones that had been used in

phenotypic screens to find inhibitors of various target enzymes (Figure 7A).<sup>61–64</sup> We employed a modified version of the cell-based, fluorometric Cresswell assay for ERAD pathway activity.<sup>65</sup> Freeze and co-workers have previously used the Cresswell assay in NGLY1-deficient cell lines as a readout of NGLY1 activity.<sup>66</sup> We stably transfected K562 cells with a de-N-glycosylation-dependent Venus (ddVenus) reporter. Mutated to be misfolded and with a site for N-glycosylation, ddVenus is translocated to the cytosol via the ERAD machinery, where deglycosylation by NGLY1 converts the target Asn residue to an Asp residue that is required for fluorescence (Figures 7B and S5). Inhibition of NGLY1 would prevent ddVenus from properly folding, thereby decreasing fluorescence in this assay. A proteasome inhibitor (e.g., carfilzomib, 1  $\mu\text{M}$ ) must be included in this assay to prevent rapid degradation of ddVenus by the ubiquitin–proteasome pathway.

We incubated these reporter cells with the library compounds for 6 h and then quantified fluorescence by flow cytometry. We identified a peptide vinyl sulfone, WRR139 (Figure 7C), as a hit, which we validated by resynthesis and dose–response analysis using the same Cresswell assay. In this assay, WRR139 had an  $\text{IC}_{50}$  of 5.5  $\mu\text{M}$  (Figure 7D), which was similar to that of Z-VAD-fmk (4.4  $\mu\text{M}$ ). The library contained other peptide vinyl sulfones of similar structure to WRR139 that were inactive (Figure 7C),

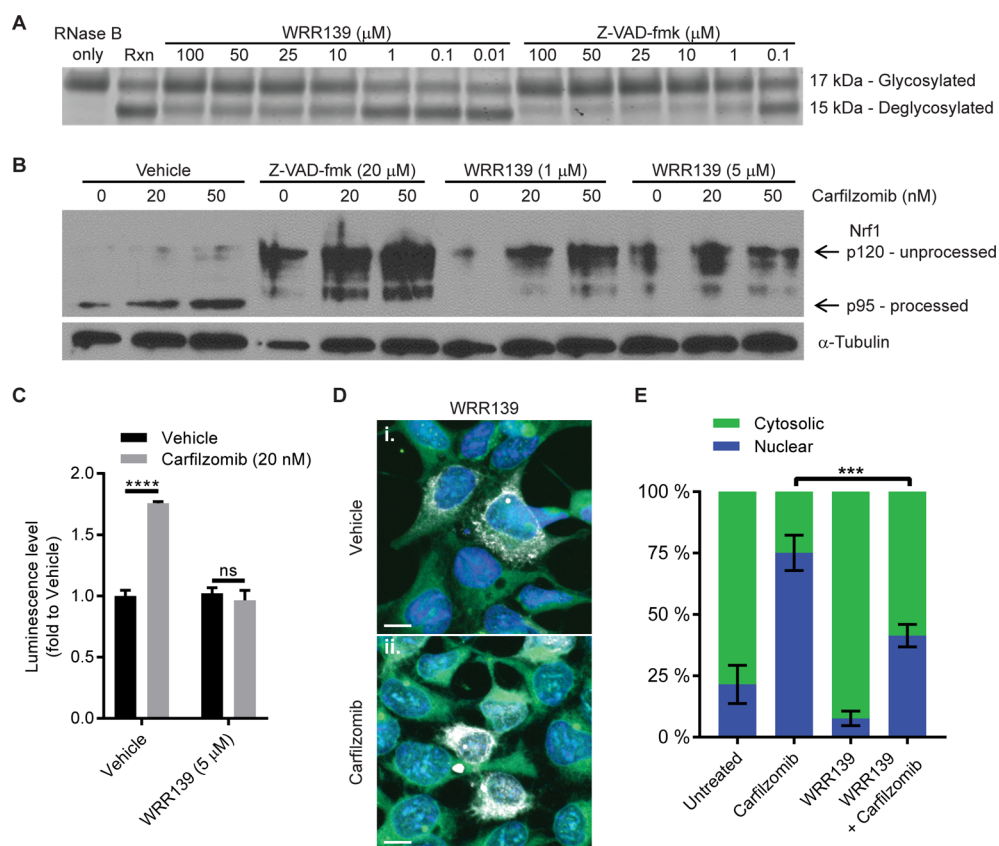


**Figure 8.** WRR139 inhibits NGLY1 *in vitro* and impairs processing of Nrf1 in cells. (A) Recombinant NGLY1 (3.75 μg) was incubated with WRR139 or Z-VAD-fmk for 60 min at 37 °C, at which time denatured and S-alkylated RNase B (1.7 μg) was added. The mixture was incubated for 60 min at 37 °C before separation by SDS–PAGE and Coomassie staining. RNase B only = no NGLY1, no inhibitor; Rxn = no inhibitor; all other lanes: inhibitor + Rxn. (B) HEK293 cells overexpressing human C-terminal 3xFLAG-tagged Nrf1 were treated with NGLY1 inhibitor Z-VAD-fmk or WRR139 for 18 h prior to treatment with carfilzomib (100 nM, 2 h). Nrf1 was visualized as described in Figure 2B. (C) Luciferase assay as described in Figure 5B using HEK293 cells overexpressing human C-terminal 3xFLAG-tagged Nrf1. The cells were treated with WRR139 (5 μM) for 5 h prior to treatment with carfilzomib (20 nM). Data for untreated cells are recapitulated from Figure 5B for comparison. (D) Immunofluorescence microscopy images of HEK293 cells overexpressing human C-terminal 3xFLAG-tagged Nrf1 that were treated with WRR139 (20 μM) for 5 h prior to treatment with vehicle (i) or carfilzomib (20 nM, ii) for 2 h. The cells were recovered in fresh medium for 1 h prior to fixation and imaging. Nrf1 immunoreactivity is indicated in white, autofluorescence is shown in green, and DAPI stained nuclei are in blue. Scale bars = 10 μm. (E) Quantitation of Nrf1 staining was accomplished by calculating the overlap of the white channel (Nrf1) with the blue channel (nucleus) and comparing it to the overall Alexa Fluor 647 signal, which was set to 100%. The difference gave the amount of Nrf1 staining outside the nucleus (green bar) and inside the nucleus (blue bar). Quantitation was performed using 5 images (125 × 75 μm) per condition and averaged. Data for untreated cells are recapitulated from Figure 3D for comparison. Error bars represent one standard deviation from the mean. \*\*\*\**p* < 0.0005, \*\*\*\**p* < 0.00005, ns = not significant.

suggesting that WRR139's activity is not simply due to its electrophilic warhead.

**WRR139 Disrupts the Processing, Localization, and Activation of Nrf1.** The Cresswell assay reports on all components of the ERAD pathway, thus it was important to confirm that WRR139 acts directly on NGLY1. Toward this end, we employed a biochemical assay with recombinant human NGLY1 (rhNGLY1, Figure S6A) expressed in Sf9 insect cells and denatured and S-alkylated RNase B as a glycoprotein substrate.<sup>67</sup> De-N-glycosylation of RNase B by NGLY1 was monitored by the change in its migration by SDS–PAGE from 17 kDa to 15 kDa (Figures 8A, S6B). We incubated rhNGLY1 with various doses of WRR139 or Z-VAD-fmk for 60 min, then added RNase B, and incubated the mixture for 1 h before analyzing the sample by SDS–PAGE. As shown in Figure 8A, both compounds showed dose-dependent inhibition of RNase B deglycosylation.

We next assessed the effects of NGLY1 inhibition by WRR139 on Nrf1 processing. HEK293 cells overexpressing C-terminal 3xFLAG-tagged Nrf1 were treated either with Z-VAD-fmk (20

μM) or with WRR139 (1 or 5 μM) for 18 h before adding various doses of carfilzomib for 6 h. The cells were lysed and analyzed by Western blotting. As shown in Figure 8B, both NGLY1 inhibitors blocked processing of Nrf1 from the p120 to p95 form. Similarly, WRR139 also inhibited activation of the ARE-dependent luciferase reporter in the presence of carfilzomib (Figure 8C), and, as found earlier for Z-VAD-fmk, WRR139 treatment together with carfilzomib caused a redistribution of Nrf1 immunoreactivity away from the nucleus (Figure 8D,E). Finally, we tested the potential off-target activity of WRR139 against the executioner caspases 3 and 7, which, once activated, induce apoptosis.<sup>68–70</sup> At concentrations up to at least 5 μM, the maximum dose used in any of our studies except for immunofluorescence microscopy, no caspase inhibitory activity was observed (Figure S7). This compares favorably to the minimum concentrations of Z-VAD-fmk needed to inhibit the caspases. However, at 10 μM WRR139 did show partial inhibition of caspases 3 and 7, suggesting an upper limit on usable doses of this compound when caspase activity is of concern.

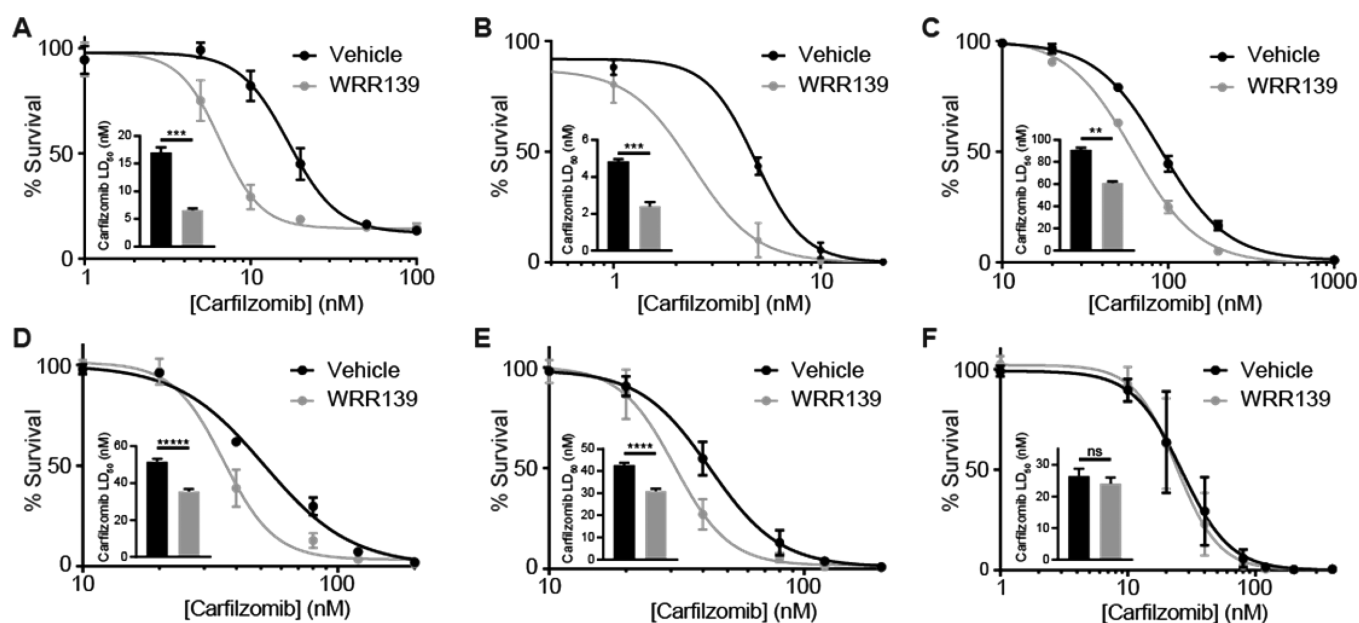


**Figure 9.** Inhibition of NGLY1 by WRR139 potentiates cytotoxicity of carfilzomib against MM and T-ALL cell lines in an NGLY1-dependent manner. (A, B, C) U266, H929, and Jurkat cells, respectively, were treated with either vehicle or WRR139 (1  $\mu$ M) and carfilzomib for 24 h. Remaining viable cells were compared to vehicle control using the CellTiter-Glo 2.0 assay,  $n = 3$ . (D, E, F) HeLa CRISPRi cells with stably expressing sgGAL4-4, sgNrf1, and sgNGLY1, respectively, were treated as in panels A, B, and C,  $n = 4$ . Error bars in A–F represent one standard deviation from the mean. Inset: The LD<sub>50</sub> of carfilzomib with cotreatment with vehicle (black) or WRR139 (gray). Error bars represent standard error. \*\* $p < 0.005$ , \*\*\* $p < 0.0005$ , \*\*\*\* $p < 0.00005$ , \*\*\*\*\* $p < 0.000005$ , ns = not significant.

**WRR139 Potentiates the Cytotoxicity of Carfilzomib in an NGLY1-Dependent Manner.** Next, we tested WRR139's ability to potentiate carfilzomib's toxicity in various leukemia cell lines: U266 and H929 MM cells and Jurkat T-ALL cells. First, we confirmed that treatment of these cell lines with 1  $\mu$ M WRR139 alone has no effect on cell viability (Figure S8). Survival of U266 and H929 cells cotreated with WRR139 and carfilzomib was significantly decreased after 24 h compared to cells treated with carfilzomib alone (Figure 9A,B). Jurkat cells also showed a significant reduction in survival when treated with both WRR139 and carfilzomib compared to carfilzomib alone (Figure 9C). This reduction in survival represented 2.6-fold, 2.0-fold, and 1.5-fold reductions in carfilzomib's LD<sub>50</sub> for U266, H929, and Jurkat cells, respectively. Interestingly, the U266 cell line is considered to be somewhat resistant to proteasome inhibition compared to other MM lines, such as H929, and this is borne out in our LD<sub>50</sub> measurements (Figure 9A,B). These cells were the most responsive to the potentiating effects of WRR139.

To confirm that WRR139's potentiating activity is directly due to NGLY1 inhibition, we measured carfilzomib's LD<sub>50</sub> in the presence or absence of WRR139 in HeLa cells with the CRISPRi backgrounds described above. In CRISPRi HeLa cells with the negative control sgGAL4-4, WRR139 potentiated carfilzomib toxicity as observed with the above leukemia cells (Figure 9D). HeLa cells with a Nrf1 knockdown behaved similarly (Figure 9E), likely due to the incomplete knockdown in these cells (Figure S3). Importantly, HeLa cells with a stable NGLY1 knockdown background showed no potentiation of carfilzomib toxicity by WRR139 (Figure 9F). These data suggest that effects of WRR139 on proteasome inhibitor potency are due to inhibition of NGLY1 and not another cellular target.

## DISCUSSION

The proteasome bounce-back response mediated by Nrf1 involves complex processing steps that have been poorly

understood. Our results demonstrate that de-N-glycosylation of Nrf1 by NGLY1 is central to the process. In cells lacking NGLY1 activity, Nrf1 was misprocessed, mislocated, and inactive. Accordingly, NGLY1 knockdown confers higher sensitivity to proteasome inhibitors and a reduced activation of PSM gene bounce-back compared to WT cells. These results solidify a biological link between NGLY1 activity and regulation of proteostasis.

While it is clear that NGLY1 and DDI2 both act on Nrf1, the order of processing events is still unconfirmed. Koizumi and co-workers found that in the absence of DDI2 de-N-glycosylation still occurs.<sup>33</sup> Prior to the discovery of DDI2's role, Sha and Goldberg showed in Nrf1, and Steffen et al. showed in an isoform of Nrf1 called TCF11, that de-N-glycosylation precedes the proteolytic cleavage event that releases Nrf1 from the ER membrane.<sup>29,71</sup> It has also been shown that Nrf3, a paralogue of Nrf1 that is similarly targeted to the ER and processed before activation, is deglycosylated prior to nuclear localization.<sup>72</sup> Recently, Kobayashi and co-workers demonstrated that the nuclear localization of Nrf3 also requires cleavage by DDI2.<sup>73</sup> Here, we observed that Nrf1 accumulates at the ER in NGLY1-null cells, suggesting that DDI2 is unable to cleave Nrf1 from the ER membrane without its prior de-N-glycosylation. We propose a Nrf1 activation pathway that includes the step of de-N-glycosylation by NGLY1 prior to proteolytic cleavage, and subsequent release from the ER, by DDI2 (Figure 1A). However, there are other possible explanations for our data. For example, there could be simultaneous or coordinated action of both NGLY1 and DDI2 on Nrf1. Our results in Figure 2E showing that treatment of the p120 form of Nrf1 produced in *Ngly1*<sup>-/-</sup> MEFs with Endo H leads to a single band that resembles the fully processed p95 form could indicate that there is active DDI2 in the cell lysate. Alternatively, it is possible that DDI2 can cleave Nrf1 with the N-glycans present but without causing the release



of Nrf1 from the ER such that it is held in a complex at the ER membrane, possibly dependent on glycosylation status.

Failure to de-N-glycosylate Nrf1 would likely inactivate the transcription factor even if it was released from the ER membrane. A glycosylated NST domain could undermine the correct folding of Nrf1, resulting in its inability to interact with Maf cofactors, DNA, or other components of the transcriptional machinery (Figure 1B). Notably, excessive amounts of Nrf1 will aggregate when the proteasome is completely shut down, according to a recent report.<sup>31</sup> Since our results demonstrate that proteasome bounce-back is diminished in cells that lack functional NGLY1, it is possible that the unprocessed form of Nrf1 trapped in the ER might also form aggregates due to lack of proteasome activity.

To date, the ubiquitin–proteasome pathway has proven to be an effective target for treatment of MM, but there is much interest in broadening the range of cancers amenable to proteasome inhibitor therapy. One approach is to combine proteasome inhibitors with drugs that target other aspects of the ubiquitin–proteasome pathway or the broader processes that feed into it, such as ERAD.<sup>14</sup> The essentiality of NGLY1 for the Nrf1-mediated bounce-back response elevates this enzyme as a possible target for cotherapy with proteasome inhibitors. Unlike Nrf1, whose druggability is questionable, NGLY1 is quite amenable to inhibition with cell penetrant small molecules. From a relatively small library of cysteine protease inhibitor-like compounds we identified one, WRR139, which inhibits NGLY1 in cultured cells, disrupts Nrf1 function, and potentiates the cytotoxicity of carfilzomib. Unlike Z-VAD-fmk, WRR139 does not inhibit caspases 3 and 7 at concentrations used for NGLY1 inhibition (<10  $\mu$ M) and is therefore a valuable new tool compound for NGLY1 research.

Importantly, there is a rare autosomal-recessive disorder characterized by inactivating mutations in both alleles of the NGLY1 gene.<sup>74,75</sup> Patients with NGLY1 deficiency experience a variety of severe pathologies, such as developmental delays, movement disorders, seizures, lacrimation, liver abnormalities, delayed bone age, and neurodegeneration.<sup>76,77</sup> These conditions are strikingly similar to phenotypes observed in mice with tissue-specific inactivation of the Nrf1 gene.<sup>78–81</sup> As well, global Nrf1 knockout in mice leads to embryonic lethality late in gestation,<sup>82</sup> as does global Ngly1 knockout.<sup>83</sup> We suggest that pathologies associated with NGLY1 deficiency may, in part, derive from a loss of Nrf1 function.

## ■ ASSOCIATED CONTENT

### 📄 Supporting Information

The Supporting Information is available free of charge on the ACS Publications website at DOI: 10.1021/acscentsci.7b00224.

Additional figures, detailed procedures for all experiments, specifics for reagents and instruments used, details on all plasmids and primers used, and synthesis details of WRR139 (PDF)

## ■ AUTHOR INFORMATION

### Corresponding Author

\*E-mail: bertozzi@stanford.edu.

### ORCID

Matthew Bogoy: 0000-0003-3753-4412

Senthil K. Radhakrishnan: 0000-0002-5211-9498

Carolyn R. Bertozzi: 0000-0003-4482-2754

## Author Contributions

‡F.M.T. and U.I.M.G.-D. contributed equally.

## Notes

The authors declare no competing financial interest.

## ■ ACKNOWLEDGMENTS

We thank Matt, Kristen, and Grace Wilsey, Kevin Lee, and Ray Deshaies for foundational discussions, Jonathan Weissman for providing dCas9-KRAB cell lines and sgRNA plasmids, Theresa McLaughlin at the Stanford University Mass Spectrometry facility for sample analysis, and Peter Cresswell for the gift of the ddVenus reporter. U.I.M.G.-D. was supported by a postdoctoral fellowship from the German Research Foundation (DFG, GE2843/1-1). R.A.F. is a Damon Runyon Postdoctoral Fellow. C.S.L. was supported by a postdoctoral fellowship from the German Research Foundation (DFG, LE3289/1-1). S.K.R. was supported by a K99/R00 Award from the National Cancer Institute (R00CA154884). This research was supported by grants from the Grace Science Foundation and by a grant to C.R.B. from the National Institutes of Health (CA200423).

## ■ REFERENCES

- (1) Ciechanover, A. The Ubiquitin-Proteasome Proteolytic Pathway. *Cell* **1994**, *79* (1), 13–21.
- (2) Adams, J. The Proteasome: Structure, Function, and Role in the Cell. *Cancer Treat. Rev.* **2003**, *29*, 3–9.
- (3) Ciechanover, A. The Ubiquitin-Proteasome Pathway: On Protein Death and Cell Life. *EMBO J.* **1998**, *17* (24), 7151–7160.
- (4) Glickman, M. H.; Ciechanover, A. The Ubiquitin-Proteasome Proteolytic Pathway: Destruction for the Sake of Construction. *Physiol. Rev.* **2002**, *82* (2), 373–428.
- (5) Schwartz, A. L.; Ciechanover, A. Targeting Proteins for Destruction by the Ubiquitin System: Implications for Human Pathobiology. *Annu. Rev. Pharmacol. Toxicol.* **2009**, *49* (1), 73–96.
- (6) Obeng, E. A.; Carlson, L. M.; Gutman, D. M.; Harrington, W. J.; Lee, K. P.; Boise, L. H. Proteasome Inhibitors Induce a Terminal Unfolded Protein Response in Multiple Myeloma Cells. *Blood* **2006**, *107* (12), 4907–4916.
- (7) Suraweera, A.; Münch, C.; Hanssum, A.; Bertolotti, A. Failure of Amino Acid Homeostasis Causes Cell Death Following Proteasome Inhibition. *Mol. Cell* **2012**, *48* (2), 242–253.
- (8) Neubert, K.; Meister, S.; Moser, K.; Weisel, F.; Maseda, D.; Amann, K.; Wiethe, C.; Winkler, T. H.; Kalden, J. R.; Manz, R. A.; et al. The Proteasome Inhibitor Bortezomib Depletes Plasma Cells and Protects Mice with Lupus-like Disease from Nephritis. *Nat. Med.* **2008**, *14* (7), 748–755.
- (9) Gomez, A. M.; Vrolix, K.; Martinez-Martinez, P.; Molenaar, P. C.; Phernambucq, M.; van der Esch, E.; Duimel, H.; Verheyen, F.; Voll, R. E.; Manz, R. A.; et al. Proteasome Inhibition with Bortezomib Depletes Plasma Cells and Autoantibodies in Experimental Autoimmune Myasthenia Gravis. *J. Immunol.* **2011**, *186* (4), 2503–2513.
- (10) Hideshima, T.; Chauhan, D.; Richardson, P.; Mitsiades, C.; Mitsiades, N.; Hayashi, T.; Munshi, N.; Dang, L.; Castro, A.; Palombella, V.; et al. NF- $\kappa$ B as a Therapeutic Target in Multiple Myeloma. *J. Biol. Chem.* **2002**, *277* (19), 16639–16647.
- (11) Lu, Z.; Hunter, T. Ubiquitylation and Proteasomal Degradation of the p21 Cip1, p27 Kip1 and p57 Kip2 CDK Inhibitors. *Cell Cycle* **2010**, *9* (12), 2342–2352.
- (12) Love, I. M.; Shi, D.; Grossman, S. R. p53 Ubiquitination and Proteasomal Degradation. *Methods Mol. Biol.* **2013**, *962*, 63–73.
- (13) Adams, J. The Proteasome: A Suitable Antineoplastic Target. *Nat. Rev. Cancer* **2004**, *4* (5), 349–360.
- (14) Deshaies, R. J. Proteotoxic Crisis, the Ubiquitin-Proteasome System, and Cancer Therapy. *BMC Biol.* **2014**, *12*:94. DOI: 10.1186/s12915-014-0094-0.

- (15) Manasanch, E. E.; Orlowski, R. Z. Proteasome Inhibitors in Cancer Therapy. *Nat. Rev. Clin. Oncol.* **2017**, *14* (7), 417–433.
- (16) Dou, Q. P.; Zonder, J. A. Overview of Proteasome Inhibitor-Based Anti-Cancer Therapies: Perspective on Bortezomib and Second Generation Proteasome Inhibitors versus Future Generation Inhibitors of Ubiquitin-Proteasome System. *Curr. Cancer Drug Targets* **2014**, *14* (6), 517–536.
- (17) Kuhn, D. J.; Chen, Q.; Voorhees, P. M.; Strader, J. S.; Shenk, K. D.; Sun, C. M.; Demo, S. D.; Bennett, M. K.; van Leeuwen, F. W. B.; Chanan-Khan, A. A.; et al. Potent Activity of Carfilzomib, a Novel, Irreversible Inhibitor of the Ubiquitin-Proteasome Pathway, against Preclinical Models of Multiple Myeloma. *Blood* **2007**, *110* (9), 3281–3290.
- (18) Muchtar, E.; Gertz, M. A.; Magen, H. A Practical Review on Carfilzomib in Multiple Myeloma. *Eur. J. Haematol.* **2016**, *96* (6), 564–577.
- (19) Lü, S.; Wang, J. The Resistance Mechanisms of Proteasome Inhibitor Bortezomib. *Biomark. Res.* **2013**, *1*:13. DOI: 10.1186/2050-7771-1-13.
- (20) Johnson, D. E. The Ubiquitin-Proteasome System: Opportunities for Therapeutic Intervention in Solid Tumors. *Endocr.-Relat. Cancer* **2015**, *22* (1), T1–T17.
- (21) Kim, H. M.; Han, J. W.; Chan, J. Y. Nuclear Factor Erythroid-2 Like 1 (NFE2L1): Structure, Function and Regulation. *Gene* **2016**, *584* (1), 17–25.
- (22) Zhang, Y.; Xiang, Y. Molecular and Cellular Basis for the Unique Functioning of Nrf1, an Indispensable Transcription Factor for Maintaining Cell Homeostasis and Organ Integrity. *Biochem. J.* **2016**, *473* (8), 961–1000.
- (23) Radhakrishnan, S. K.; Lee, C. S.; Young, P.; Beskow, A.; Chan, J. Y.; Deshaies, R. J. Transcription Factor Nrf1 Mediates the Proteasome Recovery Pathway after Proteasome Inhibition in Mammalian Cells. *Mol. Cell* **2010**, *38* (1), 17–28.
- (24) Biswas, M.; Chan, J. Y. Role of Nrf1 in Antioxidant Response Element-Mediated Gene Expression and beyond. *Toxicol. Appl. Pharmacol.* **2010**, *244* (1), 16–20.
- (25) Johnsen, Ø.; Murphy, P.; Prydz, H.; Kolsto, A. B. Interaction of the CNC-bZIP Factor TCF11/LCR-F1/Nrf1 with MafG: Binding-Site Selection and Regulation of Transcription. *Nucleic Acids Res.* **1998**, *26* (2), 512–520.
- (26) Venugopal, R.; Jaiswal, A. K. Nrf1 and Nrf2 Positively and c-Fos and Fra1 Negatively Regulate the Human Antioxidant Response Element-Mediated Expression of NAD(P)H:quinone Oxidoreductase 1 Gene. *Proc. Natl. Acad. Sci. U. S. A.* **1996**, *93*, 14960–14965.
- (27) Sankaranarayanan, K.; Jaiswal, A. K. Nrf3 Negatively Regulates Antioxidant-Response Element-Mediated Expression and Antioxidant Induction of NAD(P)H:quinone oxidoreductase 1 Gene. *J. Biol. Chem.* **2004**, *279* (49), 50810–50817.
- (28) Radhakrishnan, S. K.; den Besten, W.; Deshaies, R. J. p97-Dependent Retrotranslocation and Proteolytic Processing Govern Formation of Active Nrf1 upon Proteasome Inhibition. *eLife* **2014**, *3*, e01856.
- (29) Sha, Z.; Goldberg, A. L. Proteasome-Mediated Processing of Nrf1 Is Essential for Coordinate Induction of All Proteasome Subunits and p97. *Curr. Biol.* **2014**, *24* (14), 1573–1583.
- (30) Hagenbuchner, J.; Ausserlechner, M. J. Targeting Transcription Factors by Small compounds—Current Strategies and Future Implications. *Biochem. Pharmacol.* **2016**, *107*, 1–13.
- (31) Sha, Z.; Goldberg, A. L. Reply to Vangala et Al.: Complete Inhibition of the Proteasome Reduces New Proteasome Production by Causing Nrf1 Aggregation. *Curr. Biol.* **2016**, *26* (18), R836–R837.
- (32) Lehrbach, N. J.; Ruvkun, G. Proteasome Dysfunction Triggers Activation of SKN-1A/Nrf1 by the Aspartic Protease DDI-1. *eLife* **2016**, *5*, e17721.
- (33) Koizumi, S.; Irie, T.; Hirayama, S.; Sakurai, Y.; Yashiroda, H.; Naguro, I.; Ichijo, H.; Hamazaki, J.; Murata, S. The Aspartyl Protease DDI2 Activates Nrf1 to Compensate for Proteasome Dysfunction. *eLife* **2016**, *5*, e18357.
- (34) Zhang, Y.; Ren, Y.; Li, S.; Hayes, J. D. Transcription Factor Nrf1 Is Topologically Repartitioned across Membranes to Enable Target Gene Transactivation through Its Acidic Glucose-Responsive Domains. *PLoS One* **2014**, *9* (4), e93458.
- (35) Hirsch, C.; Blom, D.; Ploegh, H. L. A Role for N-Glycanase in the Cytosolic Turnover of Glycoproteins. *EMBO J.* **2003**, *22* (5), 1036–1046.
- (36) Suzuki, T.; Seko, A.; Kitajima, K.; Inoue, Y.; Inoue, S. Identification of Peptide:N-Glycanase Activity in Mammalian-Derived Cultured Cells. *Biochem. Biophys. Res. Commun.* **1993**, *194* (3), 1124–1130.
- (37) Suzuki, T.; Park, H.; Hollingsworth, N. M.; Sternglanz, R.; Lennarz, W. J. PNG1, a Yeast Gene Encoding a Highly Conserved peptide:N-Glycanase. *J. Cell Biol.* **2000**, *149* (5), 1039–1052.
- (38) Wang, T.; Yu, H.; Hughes, N. W.; Liu, B.; Kendirli, A.; Klein, K.; Chen, W. W.; Lander, E. S.; Sabatini, D. M. Gene Essentiality Profiling Reveals Gene Networks and Synthetic Lethal Interactions with Oncogenic Ras. *Cell* **2017**, *168* (5), 890–903.e15.
- (39) Johnsen, Ø.; Skammelsrud, N.; Luna, L.; Nishizawa, M.; Prydz, H.; Kolsto, A. B. Small Maf Proteins Interact with the Human Transcription Factor TCF11/Nrf1/LCR-F1. *Nucleic Acids Res.* **1996**, *24* (21), 4289–4297.
- (40) Chen, J.; Liu, X.; Lü, F.; Liu, X.; Ru, Y.; Ren, Y.; Yao, L.; Zhang, Y. Transcription Factor Nrf1 Is Negatively Regulated by Its O-GlcNAcylation Status. *FEBS Lett.* **2015**, *589* (18), 2347–2358.
- (41) Suzuki, T.; Huang, C.; Fujihira, H. The Cytoplasmic peptide:N-Glycanase (NGLY1) — Structure, Expression and Cellular Functions. *Gene* **2016**, *577* (1), 1–7.
- (42) Suzuki, T.; Hara, I.; Nakano, M.; Zhao, G.; Lennarz, W. J.; Schindelin, H.; Taniguchi, N.; Totani, K.; Matsuo, I.; Ito, Y. Site-Specific Labeling of Cytoplasmic Peptide:N-Glycanase by N,N'-Diacylchitobiose-Related Compounds. *J. Biol. Chem.* **2006**, *281* (31), 22152–22160.
- (43) Zhao, G.; Li, G.; Zhou, X.; Matsuo, I.; Ito, Y.; Suzuki, T.; Lennarz, W. J.; Schindelin, H. Structural and Mutational Studies on the Importance of Oligosaccharide Binding for the Activity of Yeast PNGase. *Glycobiology* **2009**, *19* (2), 118–125.
- (44) Roth, J.; Zuber, C. Quality Control of Glycoprotein Folding and ERAD: The Role of N-Glycan Handling, EDEM1 and OS-9. *Histochem. Cell Biol.* **2017**, *147* (2), 269–284.
- (45) Allen, M. D.; Buchberger, A.; Bycroft, M. The PUB Domain Functions as a p97 Binding Module in Human Peptide N-Glycanase. *J. Biol. Chem.* **2006**, *281* (35), 25502–25508.
- (46) Kamiya, Y.; Uekusa, Y.; Sumiyoshi, A.; Sasakawa, H.; Hirao, T.; Suzuki, T.; Kato, K. NMR Characterization of the Interaction between the PUB Domain of peptide:N-Glycanase and Ubiquitin-like Domain of HR23. *FEBS Lett.* **2012**, *586* (8), 1141–1146.
- (47) Huang, C.; Harada, Y.; Hosomi, A.; Masahara-Negishi, Y.; Seino, J.; Fujihira, H.; Funakoshi, Y.; Suzuki, T.; Dohmae, N.; Suzuki, T. Endo- $\beta$ -N-Acetylglucosaminidase Forms N-GlcNAc Protein Aggregates during ER-Associated Degradation in Ngly1-Defective Cells. *Proc. Natl. Acad. Sci. U. S. A.* **2015**, *112* (5), 1398–1403.
- (48) Misaghi, S.; Pacold, M. E.; Blom, D.; Ploegh, H. L.; Korbel, G. A. Using a Small Molecule Inhibitor of Peptide: N-Glycanase to Probe Its Role in Glycoprotein Turnover. *Chem. Biol.* **2004**, *11* (12), 1677–1687.
- (49) Gilbert, L. A.; Larson, M. H.; Morsut, L.; Liu, Z.; Brar, G. A.; Torres, S. E.; Stern-Ginossar, N.; Brandman, O.; Whitehead, E. H.; Doudna, J. A.; et al. CRISPR-Mediated Modular RNA-Guided Regulation of Transcription in Eukaryotes. *Cell* **2013**, *154* (2), 442–451.
- (50) Garcia-Calvo, M.; Peterson, E. P.; Leiting, B.; Ruel, R.; Nicholson, D. W.; Thornberry, N. A. Inhibition of Human Caspases by Peptide-Based and Macromolecular Inhibitors. *J. Biol. Chem.* **1998**, *273* (49), 32608–32613.
- (51) Hideshima, T.; Richardson, P.; Chauhan, D.; Palombella, V. J.; Elliott, P. J.; Adams, J.; Anderson, K. C. The Proteasome Inhibitor PS-341 Inhibits Growth, Induces Apoptosis, and Overcomes Drug Resistance in Human Multiple Myeloma Cells. *Cancer Res.* **2001**, *61* (7), 3071–3076.

- (52) Hagihara, S.; Miyazaki, A.; Matsuo, I.; Tatami, A.; Suzuki, T.; Ito, Y. Fluorescently Labeled Inhibitor for Profiling Cytoplasmic Peptide: N-Glycanase. *Glycobiology* **2007**, *17* (10), 1070–1076.
- (53) Witte, M. D.; Horst, D.; Wiertz, E. J. H. J.; van der Marel, G. A.; Overkleeft, H. S. Synthesis and Biological Evaluation of a Chitobiose-Based Peptide N-Glycanase Inhibitor Library. *J. Org. Chem.* **2009**, *74* (2), 605–616.
- (54) Kato, D.; Boatright, K. M.; Berger, A. B.; Nazif, T.; Blum, G.; Ryan, C.; Chehade, K. A. H.; Salvesen, G. S.; Bogoy, M. Activity-Based Probes That Target Diverse Cysteine Protease Families. *Nat. Chem. Biol.* **2005**, *1* (1), 33–38.
- (55) Greenbaum, D.; Medzihradzky, K. F.; Burlingame, A.; Bogoy, M. Epoxide Electrophiles as Activity-Dependent Cysteine Protease Profiling and Discovery Tools. *Chem. Biol.* **2000**, *7* (8), 569–581.
- (56) Greenbaum, D.; Baruch, A.; Hayrapetian, L.; Darula, Z.; Burlingame, A.; Medzihradzky, K. F.; Bogoy, M. Chemical Approaches for Functionally Probing the Proteome. *Mol. Cell. Proteomics* **2002**, *1* (1), 60–68.
- (57) Bogoy, M.; Verhelst, S.; Bellingard-Dubouchaud, V.; Toba, S.; Greenbaum, D. Selective Targeting of Lysosomal Cysteine Proteases with Radiolabeled Electrophilic Substrate Analogs. *Chem. Biol.* **2000**, *7* (1), 27–38.
- (58) Greenbaum, D. C.; Baruch, A.; Grainger, M.; Bozdech, Z.; Medzihradzky, K. F.; Engel, J.; DeRisi, J.; Holder, A. A.; Bogoy, M. A Role for the Protease Falcipain 1 in Host Cell Invasion by the Human Malaria Parasite. *Science (Washington, DC, U. S.)* **2002**, *298* (5600), 2002–2006.
- (59) Verhelst, S. H. L.; Bogoy, M. Solid-Phase Synthesis of Double-Headed Epoxysuccinyl Activity-Based Probes for Selective Targeting of Papain Family Cysteine Proteases. *ChemBioChem* **2005**, *6* (5), 824–827.
- (60) Wang, G.; Mahesh, U.; Chen, G. Y. J.; Yao, S. Q. Solid-Phase Synthesis of Peptide Vinyl Sulfones as Potential Inhibitors and Activity-Based Probes of Cysteine Proteases. *Org. Lett.* **2003**, *5* (5), 737–740.
- (61) Arastu-Kapur, S.; Ponder, E. L.; Fonović, U. P.; Yeoh, S.; Yuan, F.; Fonović, M.; Grainger, M.; Phillips, C. L.; Powers, J. C.; Bogoy, M. Identification of Proteases That Regulate Erythrocyte Rupture by the Malaria Parasite *Plasmodium Falciparum*. *Nat. Chem. Biol.* **2008**, *4* (3), 203–213.
- (62) Hall, C. I.; Reese, M. L.; Weerapana, E.; Child, M. A.; Bowyer, P. W.; Albrow, V. E.; Haraldsen, J. D.; Phillips, M. R.; Sandoval, E. D.; Ward, G. E.; et al. Chemical Genetic Screen Identifies Toxoplasma DJ-1 as a Regulator of Parasite Secretion, Attachment, and Invasion. *Proc. Natl. Acad. Sci. U. S. A.* **2011**, *108* (26), 10568–10573.
- (63) Child, M. A.; Hall, C. I.; Beck, J. R.; Ofori, L. O.; Albrow, V. E.; Garland, M.; Bowyer, P. W.; Bradley, P. J.; Powers, J. C.; Boothroyd, J. C.; et al. Small-Molecule Inhibition of a Depalmitoylase Enhances Toxoplasma Host-Cell Invasion. *Nat. Chem. Biol.* **2013**, *9* (10), 651–656.
- (64) Lentz, C. S.; Ordonez, A. A.; Kasperkiewicz, P.; La Greca, F.; O'Donoghue, A. J.; Schulze, C. J.; Powers, J. C.; Craik, C. S.; Drag, M.; Jain, S. K.; et al. Design of Selective Substrates and Activity-Based Probes for Hydrolase Important for Pathogenesis 1 (HIP1) from Mycobacterium Tuberculosis. *ACS Infect. Dis.* **2016**, *2* (11), 807–815.
- (65) Grotzke, J. E.; Lu, Q.; Cresswell, P. Deglycosylation-Dependent Fluorescent Proteins Provide Unique Tools for the Study of ER-Associated Degradation. *Proc. Natl. Acad. Sci. U. S. A.* **2013**, *110* (9), 3393–3398.
- (66) He, P.; Grotzke, J. E.; Ng, B. G.; Gunel, M.; Jafar-Nejad, H.; Cresswell, P.; Enns, G. M.; Freeze, H. H. A Congenital Disorder of Deglycosylation: Biochemical Characterization of N-Glycanase 1 Deficiency in Patient Fibroblasts. *Glycobiology* **2015**, *25* (8), 836–844.
- (67) Hirsch, C.; Misaghi, S.; Blom, D.; Pacold, M. E.; Ploegh, H. L. Yeast N-Glycanase Distinguishes between Native and Non-Native Glycoproteins. *EMBO Rep.* **2004**, *5* (2), 201–206.
- (68) Elmore, S. Apoptosis: A Review of Programmed Cell Death. *Toxicol. Pathol.* **2007**, *35* (4), 495–516.
- (69) McIlwain, D. R.; Berger, T.; Mak, T. W. Caspase Functions in Cell Death and Disease. *Cold Spring Harbor Perspect. Biol.* **2013**, *5* (4), 1–28.
- (70) Cullen, S. P.; Martin, S. J. Caspase Activation Pathways: Some Recent Progress. *Cell Death Differ.* **2009**, *16* (7), 935–938.
- (71) Steffen, J.; Seeger, M.; Koch, A.; Krüger, E. Proteasomal Degradation Is Transcriptionally Controlled by TCF11 via an ERAD-Dependent Feedback Loop. *Mol. Cell* **2010**, *40* (1), 147–158.
- (72) Nouhi, Z.; Chevillard, G.; Derjuga, A.; Blank, V. Endoplasmic Reticulum Association and N-Linked Glycosylation of the Human Nrf3 Transcription Factor. *FEBS Lett.* **2007**, *581* (28), 5401–5406.
- (73) Chowdhury, A. M. M. A.; Katoh, H.; Hatanaka, A.; Iwanari, H.; Nakamura, N.; Hamakubo, T.; Natsume, T.; Waku, T.; Kobayashi, A. Multiple Regulatory Mechanisms of the Biological Function of NRF3 (NFE2L3) Control Cancer Cell Proliferation. *Sci. Rep.* **2017**, *7*:12494. DOI: 10.1038/s41598-017-12675-y.
- (74) Enns, G. M.; Shashi, V.; Bainbridge, M.; Gambello, M. J.; Zahir, F. R.; Bast, T.; Crimian, R.; Schoch, K.; Platt, J.; Cox, R.; et al. Mutations in NGLY1 Cause an Inherited Disorder of the Endoplasmic Reticulum-associated Degradation Pathway. *Genet. Med.* **2014**, *16* (10), 751–758.
- (75) Suzuki, T. The Cytoplasmic peptide:N-Glycanase (Ngly1)-Basic Science Encounters a Human Genetic Disorder. *J. Biochem.* **2015**, *157* (1), 23–34.
- (76) Lam, C.; Ferreira, C.; Krasnewich, D.; Toro, C.; Latham, L.; Zein, W. M.; Lehky, T.; Brewer, C.; Baker, E. H.; Thurm, A.; et al. Prospective Phenotyping of NGLY1-CDDG, the First Congenital Disorder of Deglycosylation. *Genet. Med.* **2017**, *19* (2), 160–168.
- (77) Caglayan, A. O.; Comu, S.; Baranoski, J. F.; Parman, Y.; Kaymakçalan, H.; Akgumus, G. T.; Caglar, C.; Dolen, D.; Erson-Omay, E. Z.; Harmanci, A. S.; et al. NGLY1 Mutation Causes Neuromotor Impairment, Intellectual Disability, and Neuropathy. *Eur. J. Med. Genet.* **2015**, *58* (1), 39–43.
- (78) Kobayashi, A.; Tsukide, T.; Miyasaka, T.; Morita, T.; Mizoroki, T.; Saito, Y.; Ihara, Y.; Takashima, A.; Noguchi, N.; Fukamizu, A.; et al. Central Nervous System-Specific Deletion of Transcription Factor Nrf1 Causes Progressive Motor Neuronal Dysfunction. *Genes to Cells* **2011**, *16* (6), 692–703.
- (79) Lee, C. S.; Lee, C.; Hu, T.; Nguyen, J. M.; Zhang, J.; Martin, M. V.; Vawter, M. P.; Huang, E. J.; Chan, J. Y. Loss of Nuclear Factor E2-Related Factor 1 in the Brain Leads to Dysregulation of Proteasome Gene Expression and Neurodegeneration. *Proc. Natl. Acad. Sci. U. S. A.* **2011**, *108* (20), 8408–8413.
- (80) Xu, Z.; Chen, L.; Leung, L.; Yen, T. S. B.; Lee, C.; Chan, J. Y. Liver-Specific Inactivation of the Nrf1 Gene in Adult Mouse Leads to Nonalcoholic Steatohepatitis and Hepatic Neoplasia. *Proc. Natl. Acad. Sci. U. S. A.* **2005**, *102* (11), 4120–4125.
- (81) Kim, J.; Xing, W.; Wergedal, J.; Chan, J. Y.; Mohan, S. Targeted Disruption of Nuclear Factor Erythroid-Derived 2-like 1 in Osteoblasts Reduces Bone Size and Bone Formation in Mice. *Physiol. Genomics* **2010**, *40* (2), 100–110.
- (82) Chan, J. Y. Targeted Disruption of the Ubiquitous CNC-bZIP Transcription Factor, Nrf-1, Results in Anemia and Embryonic Lethality in Mice. *EMBO J.* **1998**, *17* (6), 1779–1787.
- (83) Fujihira, H.; Masahara-Negishi, Y.; Tamura, M.; Huang, C.; Harada, Y.; Wakana, S.; Takakura, D.; Kawasaki, N.; Taniguchi, N.; Kondoh, G.; et al. Lethality of Mice Bearing a Knockout of the Ngly1-Gene Is Partially Rescued by the Additional Deletion of the Engase Gene. *PLoS Genet.* **2017**, *13* (4), e1006696.